Research Article | Vol. 28, No. 23 / 9 November 2020 / Optics Express 34894
Optics EXPRESS

Fiber backscatter under increasing exposure to ionizing radiation

JOHANN MAX ROHR,[1,2,*] STEFAN AST,[1,2] OLIVER GERBERDING,[1,2,3] JENS REICHE,[1,2] AND GERHARD HEINZEL[1,2]

[1]Leibniz Universität Hannover, Institut für Gravitationsphysik, Callinstr. 38, 30167 Hannover, Germany
[2]Max-Planck-Institute for Gravitational Physics, Callinstr. 38, 30167 Hannover, Germany
[3]Current address: Universität Hamburg, Institute for Experimental Physics, Luruper Chaussee 175, 22761 Hamburg, Germany
[*]max.rohr@aei.mpg.de

Abstract: The Laser Interferometer Space Antenna (LISA) will measure gravitational waves by utilizing inter-satellite laser links between three triangularly-arranged spacecraft in heliocentric orbits. Each spacecraft will house two separate optical benches and needs to establish a phase reference between the two optical benches which requires a bidirectional optical connection, e.g. a fiber connection. The sensitivity of the reference interferometers, and thus of the gravitational wave measurement, could be hampered by backscattering of laser light within optical fibers. It is not yet clear if the backscatter within the fibers will remain constant during the mission duration, or if it will increase due to ionizing radiation in the space environment. Here we report the results of tests on two different fiber types under increasing intensities of ionizing radiation: SM98-PS-U40D by Fujikura, a polarization maintaining fiber, and HB1060Z by Fibercore, a polarizing fiber. We found that both types react differently to the ionizing radiation: The polarization maintaining fibers show a backscatter of about 7 ppm·m^{-1} which remains constant over increasing exposure. The polarizing fibers show about three times as much backscatter, which also remains constant over increasing exposure. However, the polarizing fibers show a significant degradation in transmission, which is reduced to about one third.

1. Introduction

The Laser Interferometer Space Antenna (LISA) will access a different frequency band of gravitational waves than ground based detectors [1,2]. Three spacecraft will form an equilateral triangle in heliocentric orbit at about 1 AU, trailing Earth by about 20°. Each spacecraft houses two individual, movable optical sub-assemblies (MOSA) to compensate the angular shifts between the spacecraft of ±1.5 ° over the orbit [3,4].

An optical connection between the two individual MOSA establishes a phase reference and is critical for the performance to be achieved after applying time-delay interferometry [5]. This connection is often referred to as "the backlink". A straightforward implementation of this is a bidirectional fiber connection [6,7]. However, Rayleigh scattering within the fibers was found to be a critical factor as the scattered light travels along the beam in the backward direction and produces a spurious interference with fluctuating phase and, therefore, limits the performance. Previous experiments suggested a linear dependency between the backscattered power and the fiber length in the order of 4 ppm·m^{-1} for short fiber lengths [7,8]. The understanding of the backscatter induced noise and the previous experimental results make it clear that a backscatter level on the same order of magnitude can be accounted for in a direct fiber connection backlink design [7]. However, in case of a significant further increase, leading to noise predictions that cannot be tuned below the picometer level requirement by changing design parameters such as

#404139 https://doi.org/10.1364/OE.404139
Journal © 2020 Received 12 Aug 2020; revised 1 Oct 2020; accepted 4 Oct 2020; published 3 Nov 2020

Optics EXPRESS

cable length, one would need to implement another, more complex backlink implementation [6]. In space, the fibers will be exposed to ionizing radiation, mostly solar protons. Assuming 1 mm aluminium equivalent shielding for the spacecraft results in an expected total ionizing dose of about 0.63 kGy reaching the fibers within the spacecraft over the extended mission duration. This total ionizing dose results from the integrated proton flux of $1.08 \cdot 10^{12}\,\mathrm{p} \cdot \mathrm{cm}^{-2}$ reaching the satellites over the extended mission duration [9,10].

Exposure to ionizing radiation can cause an increase of the fiber's attenuation depending on the fiber used. This arises from the formation of color centers within the fiber's lattice [11]. Color centers absorb a fraction of the transmitted photons and scatter these in random directions [12]. Therefore, the backscattered power may increase as a result of an increasing number of color centers within the fiber, which would be a major risk and hamper the performance of the LISA backlink. Here we report on fiber backscatter measurements addressing this risk by successively exposing the fibers to increasing amounts of ionizing radiation and measuring the backscatter afterwards. The measured backscatter and its behavior under exposure to ionizing radiation will have a determining influence on the implementation of the LISA backlink.

2. Optical setup

Fig. 1 illustrates the optical setup used to measure the fiber backscatter. The underlying measurement principle is a heterodyne Mach-Zehnder interferometer. We used a 500 mW fiber-coupled Mephisto NPRO laser from Coherent to operate the optical setup and chose a heterodyne frequency $f_{\mathrm{het}} = 5\,\mathrm{kHz}$. The laser preparation generates two beams: the sigal beam (S) and the local oscillator (LO). Both beams pass a polarizer with an extinction ratio of 10^8 and leave the laser preparation in the s-polarized state.

A photo detector placed in one of the interferometers' output ports detects an optical signal corresponding to the following voltage [13]:

$$U_{\mathrm{PD}} = k \cdot (A_{\mathrm{DC}} + A_{\mathrm{AC}} \cdot \cos(\omega_{\mathrm{het}} t + \varphi)) \tag{1}$$

In this equation k is a proportionality constant combining the properties of the photo detector and ω_{het} the angular heterodyne frequency. A_{DC} describes the mean optical power impinging onto the photo detector, whilst A_{AC} describes half the difference between maximum and minimum optical power on the photo detector. These are given as:

$$A_{\mathrm{DC}} = \rho^2 P_1 + \tau^2 P_2 \tag{2}$$

$$A_{\mathrm{AC}} = \rho\tau\sqrt{\eta P_1 P_2}. \tag{3}$$

Here, P_1 and P_2 denote the optical powers of the interfering beams in front of the recombining beamsplitter which has an amplitude reflectivity ρ and transmittivity τ. Whilst η denotes the heterodyne efficiency, which is a measure of the interference quality, e.g. mode and polarization overlap.

During the measurement campaign we investigated two different fiber types: A polarization maintaining fiber (PM) - SM98-PS-U40D by Fujikura and a polarizing fiber (PZ) - HB1060Z by Fibercore. The former is the successor product of the fiber type used in LISA Pathfinder [14], the latter is an alternative to PM fibers due to its polarizing properties and thus a possible remedy to address the polarization fluctuations observed in LISA Pathfinder [15] and LISA bread boarding [16]. All fibers under test had no jacket, a length $L = 4\,\mathrm{m}$ and used FC/APC connectors to minimize spoiling of the measurement by a reflection at the fiber interface. In all measurements the s-polarized signal beam was coupled into the slow axis of the fiber under test and all fiber couplers were aligned such, that out coupled light was also s-polarized. A residual coupling of light into the fast axis of the fibers due to small misalignments was discarded and found to be negligible for the here presented analysis.

Optics EXPRESS

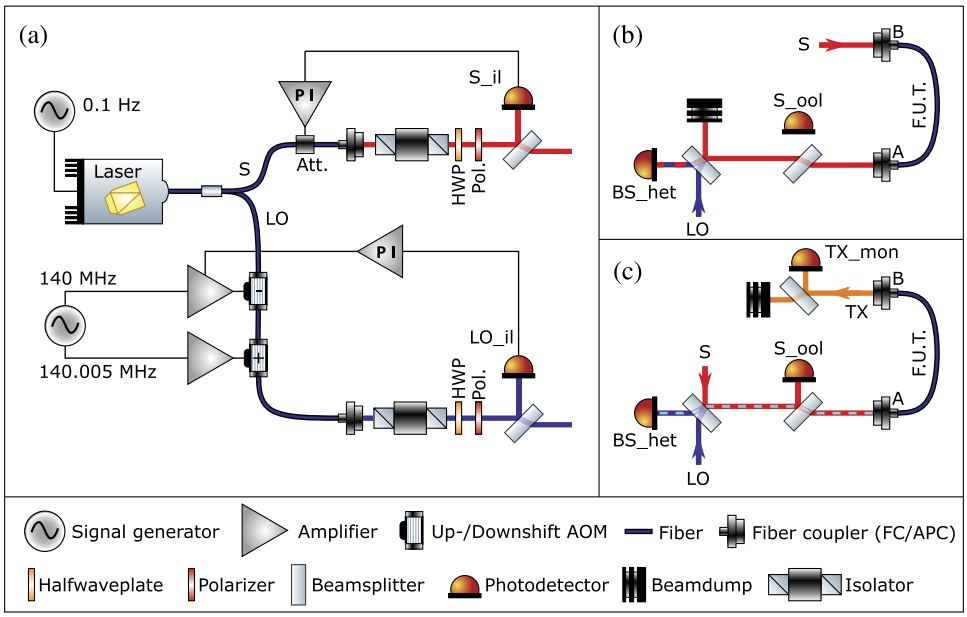

Fig. 1. Simplified sketch of the experimental setup used to measure the backscatter. Part (a) shows the laser preparation. The light emitted by a Nd:YAG laser is split into two beams: The signal beam (S) and the local oscillator (LO). With two acousto optic modulators the LO is shifted by 5 kHz with respect to S. Both beams are stabilized in amplitude using a PI-controller and one of the AOMs or a voltage controlled optical attenuator, respectively. Part (b) shows the "calibration mode", here S is coupled into the fiber under test at port B. The LO is then aligned to the beam transmitted through the fiber which resembles the mode of the backscattered light. The measured signal at the photo detector BS_het is used to calculate the heterodyne efficiency. The last measurement step, the "backscatter mode" is depicted in part (c). Here the backscattered light (dashed line) interferes with the LO and with the resulting amplitude measured on the photo detector BS_het the backscattered power is reconstructed.

Three fiber coils have been prepared for the measurements (C1, C2, C3) and each coil hosts four fibers, two of each type. The fiber assignment to each coil is depicted in Table 1. However, the fiber PM3 was damaged during handling and is therefore excluded from the evaluation. A measurement consists of two steps: The first step is the so called "calibration mode" as shown in Fig. 1(b). In this mode the signal beam is transmitted through the fiber under test from port B to port A. This is used to maximize the heterodyne efficiency η and measure it using the photo detector BS_het. This is followed by a swap to the "backscatter mode" which is depicted in Fig. 1(c). In this mode the backscatter signal is measured by injecting light into port A and amplifying the backscattered signal with the LO. The resulting heterodyne signal is measured on the photo detector BS_het. In addition, the transmitted power is monitored with

Table 1. Assignment of the fibers to the different coils. This also includes the planned radiation for the given coils.

Coil	PM fibers	PZ fibers	Irradiation
C1	PM1, PM2	PZ1, PZ2	Both
C2	PM3, PM4	PZ3, PZ4	Gamma
C3	PM5, PM6	PZ5, PZ6	Neutron

Optics EXPRESS

the photo detector TX_mon. A conservative measurement of backscatter was performed by stimulating the worst case scenario of a temperature varying fiber. To achieve this the fibers were wound on aluminium coils for better thermal contact which, however, also results in undesired mechanical stress due to the thermal expansion of the aluminium. As mechanical stress can result in additional transmission losses [17,18] the backscattered power might increase in consequence. The modulation of temperature and mechanical stress can generally also influence the polarization within the fiber, but such influences are small in PM fibers and not relevant for the measurements presented here, because we only use the slow-axis and any stress or temperature effect would need to cross couple large amounts of light into the fast-axis to generate relevant effects.

The temperature of the fiber coil was varied sinusoidal by ±1 K around the mean temperature $T_{\mathrm{coil}} = 21\,^{\circ}\mathrm{C}$. The temperature modulation was applied at a frequency of 0.02 Hz. Furthermore, a continuous sweep of the laser frequency was performed to change the interference condition between color centers within the fiber which act as spurious etalons, creating a speckle-like pattern. This frequency sweep was performed with a period of 10 s and a change of the laser frequency by about 26 MHz, which equals the free spectral range of a cavity of the fiber length.

3. Irradiation

The exposure levels were chosen in accordance to [10] such that at least the expected levels for the extended mission duration are reached. Although the key contributions to exposure in space are from solar protons, we used gamma and neutron irradiation, due to availability, gamma for the ionization and neutrons for the displacement effects, to mimic protons. The target exposures are

$$D_{\mathrm{ref}} = 0.63\,\mathrm{kGy} \tag{4}$$

$$\Phi_{\mathrm{ref}} = 1.08 \cdot 10^{12}\,\mathrm{n \cdot cm^{-2}} \tag{5}$$

for gamma and neutron irradiation, respectively. A Co-60 source was used to provide the gamma irradiation with a dose rate applied to the fibers under test of $\dot{D} = 340\,\mathrm{Gy{\cdot}h^{-1}}$. The neutrons were generated in a cold deuterium-tritium fusion with a flux rate $\dot{\Phi} = 1.26 \cdot 10^{11}\,\mathrm{n{\cdot}cm^{-2}{\cdot}h^{-1}}$. Both types of exposure were performed at the facilities of Fraunhofer Institute for Technological Trend Analysis (INT).

To measure the backscatter of the fibers under test for the intermediate values, the radiation process was interrupted by a measurement run for all fibers on the radiated coil. These measurements were performed within two hours after interrupting the exposure to keep annealing effects low. Thus, the time between interrupting the exposure and performing the backscatter measurement varies for the different fibers. The intended irradiation for the different coils is denoted in Table 1, where "both" indicates that the fibers under test were first exposed to gamma irradiation up to the maximum tested value and afterwards were exposed to the neutrons.

4. Results

4.1. Data evaluation

Using the heterodyne amplitude $U_{\mathrm{AC,cal}}$ obtained in the calibration mode measurement on the photo detector BS_het, the heterodyne efficiency of the interferometer can be calculated using Eq. (3), and is given as

$$\eta = \frac{1}{R_{\mathrm{TIA}}^2 \mathcal{R}^2} \cdot \frac{U_{\mathrm{AC,cal}}^2}{4 P_{\mathrm{LO}} P_{\mathrm{cal}} \tau^2 \rho^2} \tag{6}$$

where P_{LO} and P_{cal} are the powers of the local oscillator and the calibration beam, respectively. These are measured in front of the recombination beamsplitter. Furthermore, R_{TIA} represents the feedback resistor used in the transimpedance amplifier and $\mathcal{R}$ describes the responsivity of the

Optics EXPRESS

photo diode. Using the calculated heterodyne efficiency and the heterodyne amplitude measured in the backscatter mode, the backscattered power is reconstructed to

$$P_{\mathrm{bs}} = \frac{U_{\mathrm{AC,bs}}^2}{R_{\mathrm{TIA}}^2 \mathcal{R}^2} \cdot \frac{1}{4\eta P_{\mathrm{LO}} \rho^2 \tau^2 \tau_{\mathrm{pp}}^2}. \tag{7}$$

Here, $U_{\mathrm{AC,bs}}$ denotes the measured heterodyne amplitude in the backscatter mode measured on the photo detector BS_het. The backscattered signal propagates through an additional beamsplitter which is taken into account by the factor τ_{pp}. For comparison purposes, the backscattered power P_{bs} is scaled with the power transmitted through the fiber P_{TX}. This yields a relative value in parts-per-million for the backscattered power. The backscatter measurements were performed with heterodyne efficiencies around $\eta \simeq 0.5$ which were achieved during calibration.

A time-series of a typical measurement is shown in Fig. 2. This clearly depicts the random behavior of the scattering within the fiber. Both fiber temperature and laser frequency modulation change the interference condition between color centers within the fiber which results in the shown behavior of the backscattered power. We use the peak value observed over the measurement time to describe the given measurement; in the case shown this is 10.4 ± 2.7 ppm.

The measurement uncertainty is calculated using propagation of uncertainty [19,20] given as

$$s_X = \sqrt{\sum_k \left(\frac{\partial X}{\partial v_k}\right)^2 s_{v_k}^2}. \tag{8}$$

In this equation s_X is the uncertainty of the value X. v_k are the variables the size X depends on and s_{v_k} are the corresponding uncertainties. This is performed twice, first for the heterodyne

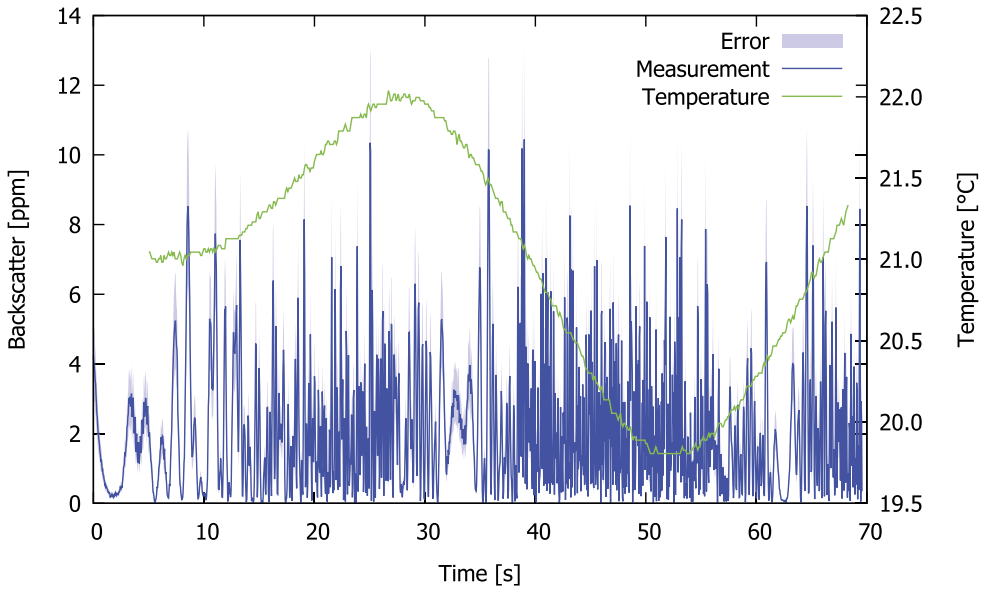

Fig. 2. Typical time-series of the backscatter measurement with active temperature and frequency modulation: Here, the random scattering behavior within the fiber is clearly visibly. The maximum value of this time-series is used to describe the given measurement step. In this case the measurement results in a backscatter of 10.4 ± 2.7 ppm. The temperature modulation of the fiber coil is depicted as well. The missing data at the beginning and the end of the temperature time-series is a result of manually starting and stopping the two involved systems.

Optics EXPRESS

efficiency (s_η) and afterwards for the backscattered power ($s_{P_{\mathrm{LO}}}$), as the latter depends on the former.

4.2. Polarization-maintaining fiber

Fig. 3 shows the results of the measurements with the PM fibers, divided in three columns. These columns show the results for the different ways the fibers were exposed to radiation: The left column shows the data taken after exposure to gamma radiation, the center column shows the measurements made after exposure to neutrons, and the right column shows the data for the fibers that were first exposed to the full dose of gamma radiation and then had an additional exposure to neutrons. The upper row of the plot shows the respective backscatter measurement while the lower row depicts the measurement of the transmitted power (with only minimal variation). The peak backscatter values for the three measurement groups are all overlapping within the respective measurement error: 17.1 ± 4.8 ppm in case of gamma radiation, 16.9 ± 4.6 ppm in case of exposure to neutrons and 20.3 ± 5.4 ppm for the combined exposure. The measurements suggest that the backscattered power remains constant over the increasing exposure for both types of radiation within the limits tested here. The transmitted power remains constant as well for both types of radiation. The coupling to the fiber is limited by not optimal mode matching, therefore, the maximum transmission measureable is around 70 % of the power impinging on the fiber's end.

4.3. Polarizing fiber

Fig. 4 shows the results of the measurement using the PZ fibers, Fibercore HB1060Z. The assignment of the columns to the different types of radiation is the same as in Fig. 3. The upper row depicts the backscatter measurements while the lower row depicts the transmitted power. For the PZ fibers the peak backscatter values are: 41.1 ± 12.4 ppm in case of exposure to gamma radiation, 44.7 ± 12.5 ppm for the exposure to neutrons and 52.3 ± 16.2 ppm in the combined case. The measurements show that, similar to the PM fibers, the backscattered power remains constant within our measurement error. However, the transmitted power decreases significantly over the increasing exposure for both types of radiation. In the combined case the transmission appears to be either constant or decreasing only marginally. This is a result of the way the combined radiation was performed and consequently dominated by the effect of the full gamma exposure beforehand.

4.4. Summary

Table 2 lists the measured backscatter peak values obtained in the different measurement groups. The worst case measurement of the PM fibers is at 25.7 ppm, which corresponds to 6.43 ppm·m^{-1}. We obtained this value by adding the measured value and the corresponding measurement error from Table 2. The PZ fibers show a higher backscatter than the PM fibers by about a factor of three, here the maximum measurement is 68.5 ppm which corresponds to 17.13 ppm·m^{-1}.

Additionally, we fitted a negative exponential distribution to all our measurements as the backscattered power follows this type of distribution [21]. This results in a value of the μ-parameter describing the measurement. The mean value of this parameter for each type of exposure and fiber and the corresponding standard deviation are also listed in Table 2. The values of the μ-parameter remained constant over the increasing exposure as well.

Optics EXPRESS

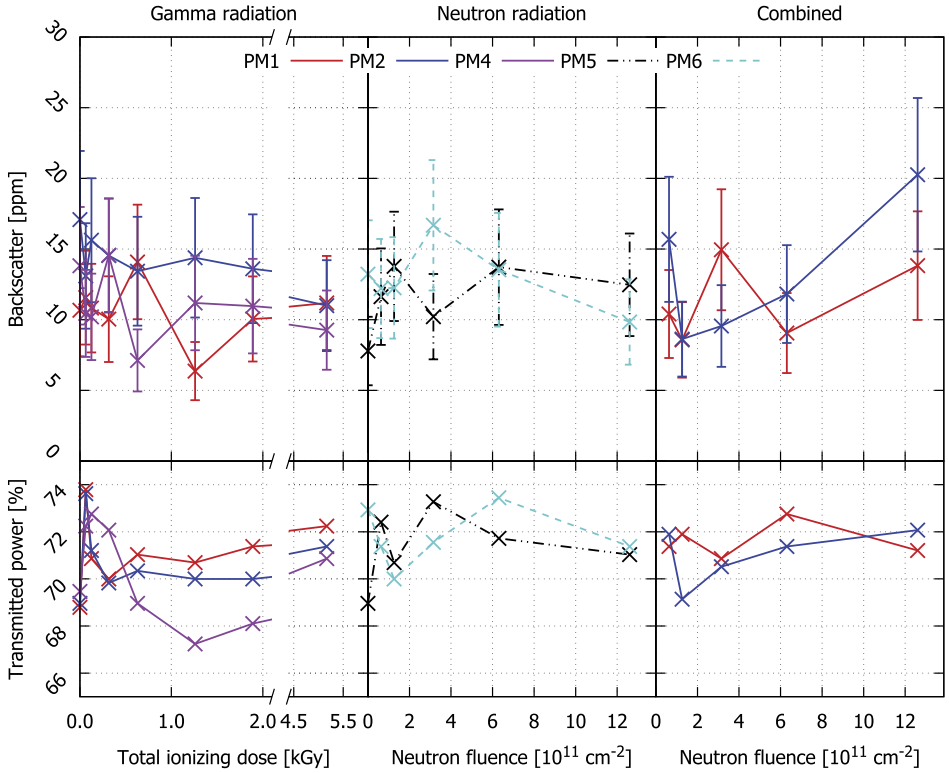

Fig. 3. Results of the measurement with the PM fibers, Fujikura SM98-PS-U40D. The upper row of plots depicts the measured backscatter and the lower row the transmission measured at the same step. The left column depicts the results after exposure to gamma radiation and the central column shows the measurements after exposure to neutrons. The right column depicts the data taken for some fibers that were first exposed to gamma radiation and afterwards exposed to neutrons. Overall, the measurements with the PM fibers do not show an increase of backscattered light within the measurement error. Moreover, the transmission remains unchanged within the measurement error.

Table 2. Highest backscatter values and mean μ-parameters of the fit to a negative exponential distribution observed during the measurement campaign. For the peak values the measurement error is added and for the μ-parameter the standard deviation of these is added. The values of the polarizing fibers are between two and three times higher than those of the polarization maintaining fibers.

	Peak backscatter [ppm]		Mean μ-parameter [ppm]	
Radiation type	PM fibers	PZ fibers	PM fibers	PZ fibers
Gamma	17.1 ± 4.8	41.1 ± 12.4	2.02 ± 1.14	6.58 ± 2.55
Neutron	16.9 ± 4.6	44.7 ± 12.5	2.11 ± 0.33	5.93 ± 1.90
Gamma+Neutron	20.3 ± 5.4	52.3 ± 16.2	2.11 ± 0.55	5.69 ± 1.99

Optics EXPRESS

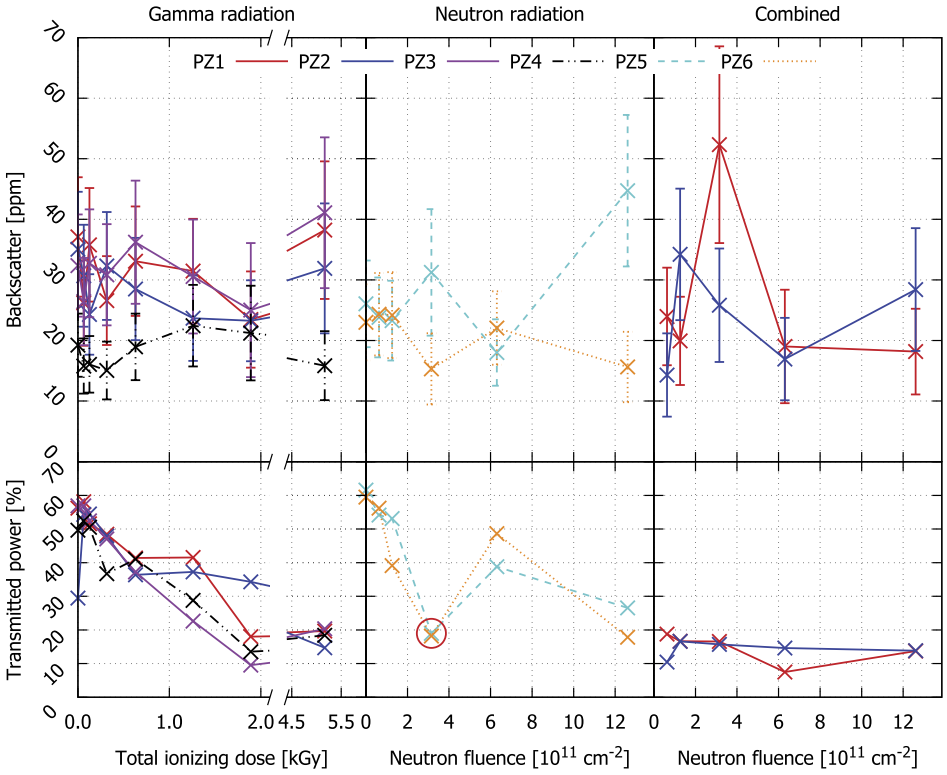

Fig. 4. Results of the measurements with the PZ fibers, Fibercore HB1060Z. Exposing these to gamma irradiation and neutrons does not cause a change of the backscattered power within our measurement accuracy. However, an increase in attenuation is observed as the transmission decreases to about one third. The transmission decrease in the "combined" case is dominated by the effect of the exposure to gamma radiation. The transmission measurements in the case of neutron radiation at $3.2 \cdot 10^{11}$ n·cm^{-2} is a measurement error (these are marked by a red circle). Excluding this measurement, the decrease of transmission is qualitatively equal to the decrease observed in the case of exposure to gamma radiation. The exposure to about 2 kGy is roughly equivalent to the full neutron exposure.

Optics EXPRESS

5. Conclusion

We have presented a first irradiation testing of the candidate LISA backlink fibers to mimic the effects of the space environment on the backscatter levels. Our measurements show that the backscattered power of the two types of optical fibers under test remains constant over increasing exposure to ionizing radiation. This implies that a bidirectional optical fiber connection, like the LISA backlink, will not be hampered additionally by an increase of backscattered power induced by radiation for the given fiber types. Furthermore, the level of backscatter observed here can be accounted for in a direct fiber backlink design and agrees with the independent measurements in [8]. Our measurements show that the polarizing fiber (Fibercore HB1060Z) show more backscatter than the polarization maintaining fiber (Fujikura SM98-PS-U40D). A probable cause for this is the internal structure of the polarizing fibers which feature a different form of stress rods than the polarization maintaining fibers. It is also possible that this is caused by the environment during the fiber drawing process [22] and a subsequent increase in color centers within the fiber.

Furthermore, we observed a decrease in transmission for the polarizing fibers which shows that this fiber type is not radiation hard. This disqualifies these as a viable alternative to the tested polarization maintaining fiber which does not show a decrease in transmission.

Funding

Deutsches Zentrum für Luft- und Raumfahrt (50 OQ 0601, 50 OQ 1301, 50 OQ 1801); European Space Agency (8586/16/NL/BW).

Acknowledgments

We gratefully acknowledge support by the European Space Agency (ESA) within the project "Phase Reference Distribution System" (8586/16/NL/BW) and the Deutsches Zentrum für Luft- und Raumfahrt (DLR) with funding from the Bundesministerium für Wirtschaft und Technologie (Project Ref. Number 50 OQ 1801, based on work done under Project Ref. Number 50 OQ 1301 and 50 OQ 0601). Furthermore, the authors gratefully acknowledge support by Jochen Kuhnhenn and Simone Schmitz from the Fraunhofer Institute for Technological Trend Analysis (INT), Euskirchen, Germany in operating the radiation facilities. The authors also would like to thank the current and former members of the "Backlink Team" for numerous useful discussions.

Disclosures

The authors declare no conflicts of interest.

References

1. K. Danzmann, "LISA — an ESA cornerstone mission for the detection and observation of gravitational waves," Adv. Space Res. **32**(7), 1233–1242 (2003).
2. O. Jennrich, "LISA technology and instrumentation," Classical Quantum Gravity **26**(15), 153001 (2009).
3. LISA Instrument Group, "LISA Payload Definition Document," Tech. Rep. ESA-L3-EST-INST-DD-001, European Space Agency (2018).
4. S. P. Hughes and F. H. Bauer, "Preliminary optimal orbit design for the laser interferometer space antenna (lisa)," (2002).
5. M. Otto, G. Heinzel, and K. Danzmann, "TDI and clock noise removal for the split interferometry configuration of LISA," Classical Quantum Gravity **29**(20), 205003 (2012).
6. K.-S. Isleif, L. Bischof, S. Ast, D. Penkert, T. S. Schwarze, G. F. Barranco, M. Zwetz, S. Veith, J.-S. Hennig, M. Tröbs, J. Reiche, O. Gerberding, K. Danzmann, and G. Heinzel, "Towards the LISA backlink: experiment design for comparing optical phase reference distribution systems," Classical Quantum Gravity **35**(8), 085009 (2018).
7. R. Fleddermann, C. Diekmann, F. Steier, M. Tröbs, G. Heinzel, and K. Danzmann, "Sub-pm$\sqrt{\text{Hz}}^{-1}$ non-reciprocal noise in the LISA backlink fiber," Classical Quantum Gravity **35**(7), 075007 (2018).
8. J. Rybizki, "LISA back-link fibre: back reflection of a polarisation maintaining single-mode optical fibre," Diploma thesis, Leibniz Universität Hannover (2011).

Optics EXPRESS

9. M. Zwetz and S. Ast, "Phase Reference Distribution System Fiber Irradiation Test Report," Tech. Rep. LISA-AEI-PRDS-RP-001, Max-Planck-Institut für Gravitationsphysik, Albert-Einstein-Institut, Teilinstitut Hannover (2019).
10. M. Millinger and P. Jiggens, "LISA Environment Specification," Tech. Rep. ESA-L3-EST-MIS-SP-001, ESA-TEC-SP-00666, European Space Agency (2017).
11. P. W. Levy, "Color centers and radiation-induced defects inAl2o3," Phys. Rev. **123**(4), 1226–1233 (1961).
12. E. J. Friebele and D. L. Griscom, "Color centers in glass optical fiber waveguides," Mater. Res. Soc. Symp. Proc. **61**, 319 (1985).
13. O. Gerberding, "Phase readout for satellite interferometry," PhD thesis, Leibniz Universität Hannover (2014).
14. C. J. Killow, E. D. Fitzsimons, M. Perreur-Lloyd, D. I. Robertson, H. Ward, and J. Bogenstahl, "Optical fiber couplers for precision spaceborne metrology," Appl. Opt. **55**(10), 2724 (2016).
15. G. Heinzel, M. Hewitson, M. Born, N. Karnesis, L. Wissel, B. Kaune, G. Wanner, K. Danzmann, S. Paczkowski, A. Wittchen, M.-S. Hartig, H. Audley, and J. Reiche, "LISA Pathfinder mission extension report for the German contribution," Tech. rep. (2020).
16. T. S. Schwarze, G. F. Barranco, D. Penkert, M. Kaufer, O. Gerberding, and G. Heinzel, "Picometer-stable hexagonal optical bench to verify LISA phase extraction linearity and precision," Phys. Rev. Lett. **122**(8), 081104 (2019).
17. E. Suhir, "Mechanical approach to the evaluation of the low temperature threshold of added transmission losses in single-coated optical fibers," J. Lightwave Technol. **8**(6), 863–868 (1990).
18. J. D. LeGrange, H. C. Ling, and D. M. Velez, "Effects of mechanical stress on the transmission properties of optical fiber packaged in a composite structure," Appl. Opt. **33**(18), 3890 (1994).
19. R. T. Birge, "The propagation of errors," Am. J. Phys. **7**(6), 351–357 (1939).
20. H. Ku, "Notes on the use of propagation of error formulas," J. Res. Natl. Bureau Standards, Sect. C: Eng. Instrumentation **70C**, 263 (1966).
21. J. W. Goodman, *Speckle Phenomena in Optics: Theory and Applications, Second Edition* (SPIE, 2020).
22. S. Sakaguchi, "Relaxation of rayleigh scattering in silica core optical fiber by heat treatment," Electron. Comm. Jpn. Pt. II **83**(12), 35–41 (2000).